

Raman Scattering Studies on *n*-Heptane under High Pressure

G. Kavitha and Chandrabhas Narayana*

Chemistry and Physics of Material Unit, Jawaharlal Nehru Centre for Advanced Scientific Research, Jakkur P.O., Bangalore 560 064, India

Received: October 27, 2005; In Final Form: March 8, 2006

High-pressure Raman scattering studies at ambient temperature are performed on *n*-heptane. We observe a liquid–solid transition around 1.5 GPa from the changes in the Raman spectra. This has been reported in earlier works. With increasing pressure, we observe large changes in the Raman modes and the spectra show a distinct change around 7.5 GPa. This marks the solid–solid transition at 7.5 GPa observed in *n*-heptane for the first time. As predicted in theoretical work, we observe dampening of methyl rotation in *n*-heptane below 7.5 GPa. With increase in pressure above 7.5 GPa we observe a definitive conversion of gauche to trans conformation in the solid phase. Upon release of pressure we do not observe any hysteresis, which suggests that the solid–solid transition takes place with no volume change or is a second-order transition. In this paper we propose this transition to be an orientational order–disorder transition driven by the dampening of the rotation of the methyl group.

1. Introduction

Long- and short-chain alkanes have various applications in industry, such as use as lubricants or as solvents. Liquid *n*-heptane mixed with isooctane has the antiknocking properties of engine fuels.¹ Since an alkyl group is present in several complex molecular systems² and forms a crucial component in systems ranging from membranes to micelles and self-assembled monolayers,³ a study of the phase diagram of linear and branched alkanes helps in the understanding of the complex phenomena in these systems. In the crystalline phase, linear alkanes exhibit interesting rotator phases, which have been shown using neutron scattering⁴ and computer simulations.⁵ There has been considerable interest in the structure and dynamics of crystalline *n*-alkanes, which have been recently studied.^{6–10}

High-pressure infrared (IR) spectroscopic investigations carried out up to a pressure of 7 GPa revealed that *n*-heptane undergoes a liquid to solid transition at ~ 1.2 – 1.5 GPa and a possible solid–solid transition at ~ 3 GPa.⁹ Recent molecular dynamic (MD) simulations on *n*-heptane have confirmed the existence of the liquid to solid transition at ~ 1.2 – 1.5 GPa, but could not show any evidence of solid–solid transition in their studies up to 7 GPa.¹⁰ The MD simulations revealed a dynamic arrest of the rotation of the methyl end groups and extensive changes in the environment around the end groups of *n*-heptane as a function of pressure in the solid phase.¹⁰ The cumulative effect of the dynamic arrest of the rotation and changes in the environment around the methyl end group could introduce a phase transition in *n*-heptane at higher pressures. In view of this and to verify the theoretical prediction, we have undertaken a comprehensive investigation of *n*-heptane under pressure at ambient temperature with Raman spectroscopy as the probe. Vibrational spectroscopy is a powerful tool for investigating the conformations and dynamics of molecules in the condensed phase, and there are inherent advantages of Raman scattering over the complementary technique of IR spectroscopy. Longi-

tudinal acoustic modes (LAM), lattice vibrations, librational modes, and other internal modes of *n*-alkanes are sensitive to intermolecular interactions in the condensed phase and are observable in Raman spectroscopy.^{11–13}

Our high-pressure studies show the expected liquid to solid transition around 1.5 GPa. We also observe the effect of dynamic arrest of the methyl end group from the behavior of the methyl torsional mode and the related vibrational mode of methyl end group below 7.5 GPa. We observe a solid to solid phase transformation above 7.5 GPa as deduced from the change in the Raman spectra above and below the transition pressure of 7.5 GPa. Upon releasing the pressure, we observe that all the modes reappear and the spectrum is similar to the increasing pressure data below 7.5 GPa. The *n*-heptane returns to the liquid phase below 1.5 GPa. We do not see any hysteresis around the 7.5 GPa transition, suggesting that the solid–solid transition in *n*-heptane is second order in nature. In this paper based on our observations, we suggest that the new phase is an orientationally disordered phase with no volume change, driven by the dampening of methyl end group.

2. Experimental Details

We have used *n*-heptane bought from Sigma-Aldrich without further purification. A Mao-Bell type piston cylinder diamond anvil cell (DAC) with a 1:6 lever arm was used to generate the pressure.¹⁴ The pressure was measured in situ using the ruby fluorescence technique.¹⁵ The experiments were carried out in a backscattering geometry using a laser excitation wavelength of 532 nm from a solid-state diode pumped Nd:YAG laser (Coherent Inc., USA) of ~ 120 mW power. The Raman spectra were recorded using a Jobin-Yvon Triax 550 and a liquid N₂ cooled CCD detector (Instrument SA, USA), the details of which can be found in ref 16.

3. Results and Discussion

n-Heptane (C₇H₁₆) crystallizes in a triclinic cell with space group *P*1̄, with crystal density 0.890 gm/cm³ and having lattice

* Corresponding author. E-mail: cbhas@jncasr.ac.in.

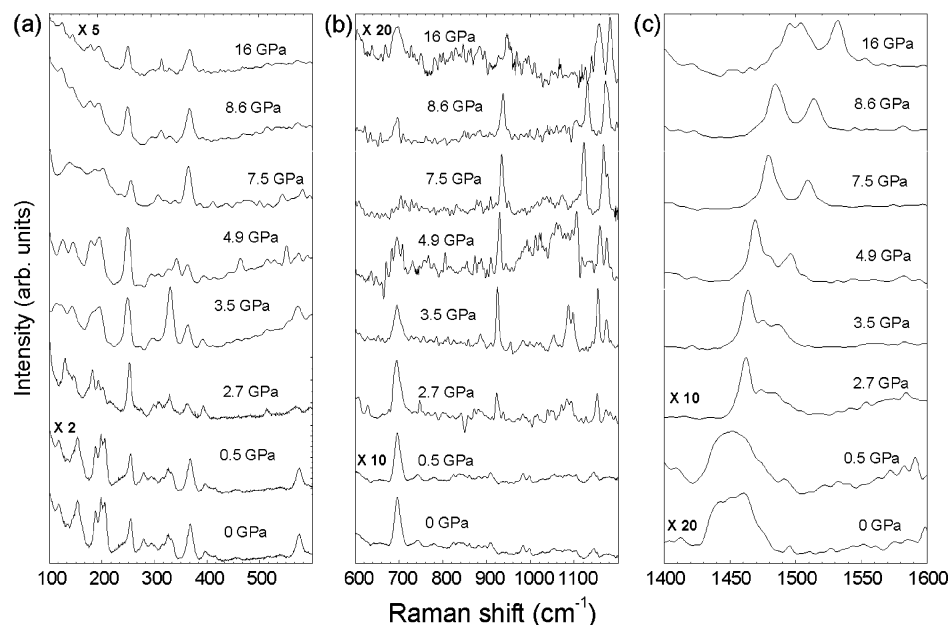


Figure 1. Raman spectra of *n*-heptane at ambient conditions and at high pressures. For clarity the spectra have been divided into three parts: (a) 100–600, (b) 600–1200, and (c) 1400–1600 cm^{-1} . The region 1200–1400 cm^{-1} is dominated by a diamond first-order peak and has not been shown.

TABLE 1: Frequency (ω) and Its Pressure Derivative ($d\omega/dP$) for the Various Raman Modes of *n*-Heptane in Three Different Phases and Their Mode Assignments

phase I (0 GPa)		phase II (1.4 GPa)		phase III (7.9 GPa)		mode assignment
ω (cm^{-1})	$d\omega/dP$	ω (cm^{-1})	$d\omega/dP$	ω (cm^{-1})	$d\omega/dP$	
115	0.8					lattice and acoustic mode
134	1.6	134	−0.8	131	0.4	lattice and acoustic mode
152	1.6	152	0.4	153	0.2	librational mode
187	−0.7	185	0.1	185	0.3	lattice and acoustic mode
198	−0.1	197	0.6			lattice and acoustic mode
205	0.3	205	−0.1	206	−0.6	lattice and acoustic mode
252	2.3	255	0.2	255	0.2	methyl rotation
278	0.5					methyl torsion
295	2.4	300	0.6			methyl torsion
313	−2.4	311	0.6	311	0.6	longitudinal acoustic
328	−2.4	330	7.2	366	4.8	librational mode
367	−1.9	364	1.5			GTTT conformer
399	−2.2	395	1.3			superposition of GTTT and TTGG
568	26.7	595	−1.5			single gauche
				693	0.9	in-phase CH_3 rocking
696	−2.3	694	0.9			in-phase CH_3 rocking
743	1.8					CH_2 rocking
818	9.4	834	6.4	858	1.4	symmetric C–C stretching
842	11.5					symmetric C–C stretching
908	4.0	926	2.6	937	2.1	CH_2 twist
985	−9.2	985	0.0			methyl rocking
1000	5.7	1018	5.4	1018	5.4	skeletal C–C stretching
1056	−4.1	1053	4.7	1053	4.7	skeletal C–C stretching
1090	2.8	1089	3.7	1106	4.7	gauche defect
				1144	1.0	trans conformer
1148	0.6	1156	3.1	1171	1.1	trans conformer
1178	0.7	1181	7.5	1181	7.5	CH_2 twisting
1442	1.3	1461	0.9	1461	0.9	asymmetric CH_2 and CH_3 bending
1453	−0.1	1473	2.0	1475	4.5	asymmetric CH_2 and CH_3 bending
1461	1.3	1483	5.5	1483	5.5	symmetric out-of-plane CH_3 bending

parameters $a = 4.15 \text{ \AA}$, $b = 19.97 \text{ \AA}$, $c = 4.69 \text{ \AA}$, $\alpha = 91.3^\circ$, $\beta = 74.3^\circ$, and $\gamma = 85.1^\circ$ at a pressure of ~ 1.2 – 1.5 GPa .¹⁰ The chain axis of each molecule makes an angle of 2° with the ab -plane and 71° with the a -axis. Figure 1 shows the Raman spectra of *n*-heptane at ambient and high pressures carried out up to 16 GPa. Table 1 shows the mode frequencies (ω), pressure derivative ($d\omega/dP$), and mode assignments of the Raman spectra of the *n*-heptane at three different phases of *n*-heptane in the 0–16 GPa pressure range. The mode assignments were based

on ref 17. We observe the liquid to solid transition around 1.5 GPa deduced from the changes in Raman spectra of *n*-heptane above and below 1.5 GPa. This has been reported earlier,^{9,10} and we will restrict our discussion to the pressure dependence of the solid phase of *n*-heptane in this paper. Since *n*-heptane is a molecular solid, the Raman spectrum shows the librational modes along with the lattice and the acoustic modes in the range 100–400 cm^{-1} , also known as external modes. The internal modes or the intramolecular vibrations are found above 250

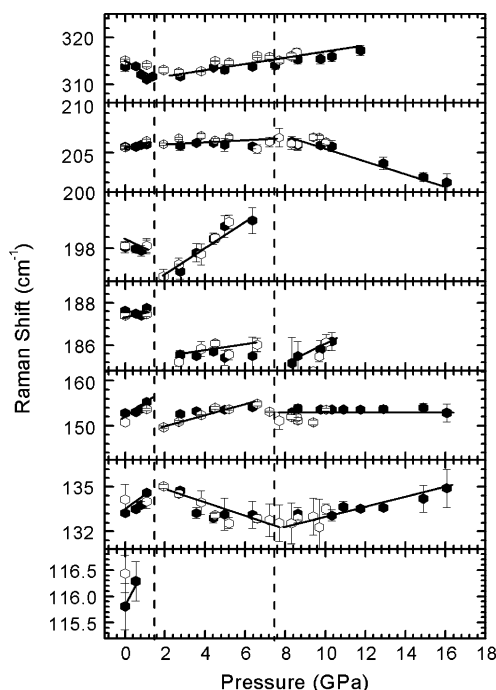


Figure 2. Behavior of external modes as a function of pressure. Filled symbols represent increasing pressure data, and open symbols represent reverse pressure data. The solid lines through the data points are linear fits to the data.

cm^{-1} . Internal modes have been grouped into (i) rotation, torsion, and rocking modes of methyl end group, (ii) vibrational modes due to gauche and trans conformations, (iii) skeletal C–C vibration modes, (iv) CH_2 stretching vibrations, and (v) CH_2 and CH_3 bending vibration modes. We discuss below the effect of the pressure on these modes and the implication of the same on the structure of *n*-heptane in the solid phase.

3.1. External Modes. In a molecular solid, where the intermolecular interactions are van der Waals, upon application of pressure we expect large changes in the lattice, acoustic, and librational modes. These modes are very sensitive to subtle transition. Figure 2 shows the pressure dependence of all the external modes observed in *n*-heptane. We observe the disappearance of the 197 cm^{-1} mode and large pressure effects on other modes of phase II above 7.5 GPa. It is interesting to note the pressure dependence of the 152 cm^{-1} mode of phase I. This corresponds to vibration followed by rotation involving atomic displacements in the direction perpendicular to the molecular long axis.¹⁰ In the solid phase this mode has very little pressure dependence. This suggests that the *n*-heptane is densely packed in the direction perpendicular to the molecular long axis. The decrease in number of lattice and acoustic modes along with changes in the mode behavior above 7.5 GPa suggests a definitive phase transition.

3.2. Internal Modes. **3.2.1. Methyl Rotation, Torsional, and Rocking Vibrational Modes.** Figure 3 shows the vibrational mode frequencies associated with methyl rotation, torsion, and rocking as a function of pressure. We observe five modes associated with the methyl end groups in this category at ambient conditions: In phase I, 252 cm^{-1} is the methyl rotation mode, 278 and 295 cm^{-1} are methyl torsional modes, and 696 and 985 cm^{-1} are methyl rocking modes.¹⁷ Molecular dynamic simulation studies suggest that the methyl end group vibrations show a considerable dampening with increase in pressure up to 7 GPa.¹⁰ As shown in Figure 3, we observe the disappearance of the methyl torsional modes. This means that the torsional mode ceases to exist above 7.5 GPa. The methyl rocking modes

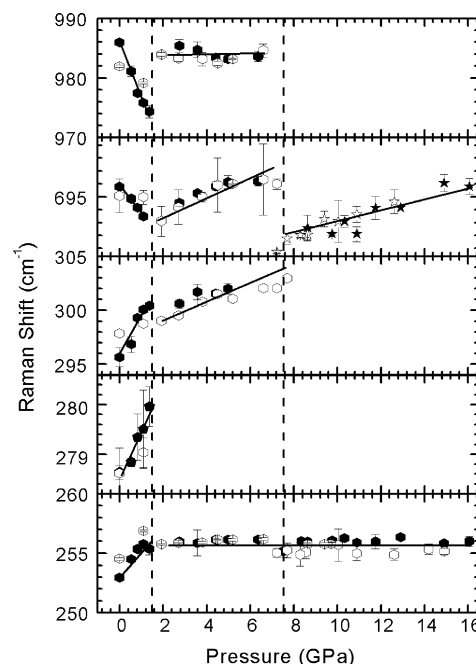


Figure 3. Vibrational modes associated with CH_3 rotation, torsional, and rocking as a function of pressure. Filled symbols represent increasing pressure data, and open symbols represent reverse pressure data. The open and filled star symbols represent the new mode above 7.5 GPa. The solid lines are linear fits to the data.

also disappear, but a new mode appears in phase III at a much lower frequency (692 cm^{-1}). These observations support the MD simulation studies;¹⁰ namely, there is considerable dampening of vibrational degree of freedom for the methyl end groups at high pressures leading to a phase transition at 7.5 GPa. It is interesting to see that 252 cm^{-1} mode (phase I) associated with methyl rotation about the long axis of the molecule does not show any pressure dependence in the solid phase. This could be due to dense packing of *n*-heptane along the *c*-axis as the pressure is increased. In IR studies of *n*-alkanes at high temperatures, in an all-trans (planar) conformation, one observes hindered rotation and twisting about the long axis, which supports our case.¹⁸

3.2.2. Vibrational Modes of Gauche and Trans Conformers. It is known that increase in pressure favors the gauche form over the trans form. This has been shown in the case of *n*-hexane along the liquid to solid transition, but no one has seen the effect of pressure at very high pressures.¹⁹ In *n*-heptane also, in the liquid to solid transition, we observe an increase in the gauche form compared to the trans form looking at the intensities of these modes. Figure 4 shows the various modes associated with the gauche and trans conformers and their pressure dependence. In the solid phase, with the increase in pressure, that is, decrease in volume, linear alkanes should show a considerable change in their gauche and trans conformers. In the case of *n*-heptane at ambient pressures we observe both single and double gauche conformers along with all-trans conformers (see Table 1). Due to the presence of a strong diamond Raman band around 1332 cm^{-1} from the DAC, we could not quantitatively measure the intensities of these modes. It is standard to look at the intensities of 1090 and 1148 cm^{-1} to ascertain the amount of gauche and trans conformers.^{20–22} In the case of *n*-hexane, low-frequency modes around $250\text{--}550\text{ cm}^{-1}$, which are related to these conformers, have been looked at to determine the conformers.¹⁹ In our case, too, the qualitative measurements of intensities of 367 (GTTT), 399 (GTTT and TTGG), and 568 cm^{-1} (single gauche) in phase I increases with increase in pressure, suggesting

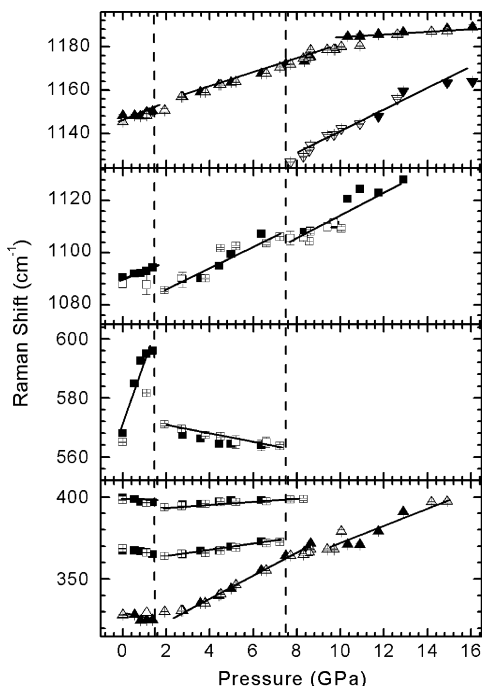


Figure 4. Vibrational modes associated with gauche and trans conformers as a function of pressure. Filled symbols represent the increasing pressure data, and open symbols represent reverse pressure data. Squares represent the gauche conformers, and triangles represent trans conformers. The solid lines are linear fits through the data.

that increase in pressure favors the gauche form as seen in *n*-alkanes.^{19,23} At pressures >5 GPa, in the solid phase, we observe that with increase in pressure there is considerable decrease in the gauche defects and increase in trans conformers. This is seen from the disappearance of 367, 399, and 568 cm⁻¹ (phase I) and the appearance of a new mode at 1144 cm⁻¹ (all trans of phase III) above 7.5 GPa. We have made a qualitative intensity measurement of the 1090 and 1148 cm⁻¹ modes of phase I. We observe an increase in intensity of the 1148 cm⁻¹ mode with a decrease in intensity of the 1090 cm⁻¹ mode. This again suggests that *n*-heptane at high pressure is tending toward an all-trans conformation.^{20–22} However, the 1090 cm⁻¹ mode persists up to 12 GPa and this mode is difficult to measure above this pressure, suggesting that there are some gauche defects still present at high pressures.

3.2.3. C–C Stretching Vibrational Modes. Figure 5 shows various C–C backbone stretching modes associated with *n*-heptane and its pressure dependence. As we increase the pressure, these modes harden in the solid phase. With a decrease in the volume at high pressures, there is an increase in the interatomic interactions, leading to a much stiffer mode. These modes are difficult to observe at pressures greater than 10 GPa due to interference from other modes in this region. The above observation also suggests that the *n*-heptane, being a linear chain, packs along the *c*-axis, which is perpendicular to the chain direction. Hence the phase transition has no effect on the behavior of these modes across the transition.

3.2.4. CH₂ Vibrational Modes. Figure 6 shows the CH₂ vibrational modes and their pressure dependence. The CH₂ rocking mode at 743 cm⁻¹ of phase I ceases to exist in the solid phase above 7.5 GPa due to restriction in the degree of freedom along the *c*-axis in the condensed phase. The CH₂ twisting modes at 908 and 1178 cm⁻¹ of phase I show considerable hardening in both the liquid phase and solid phase. The hardenings of these modes are expected due to increase in interatomic interactions in the condensed phase at higher

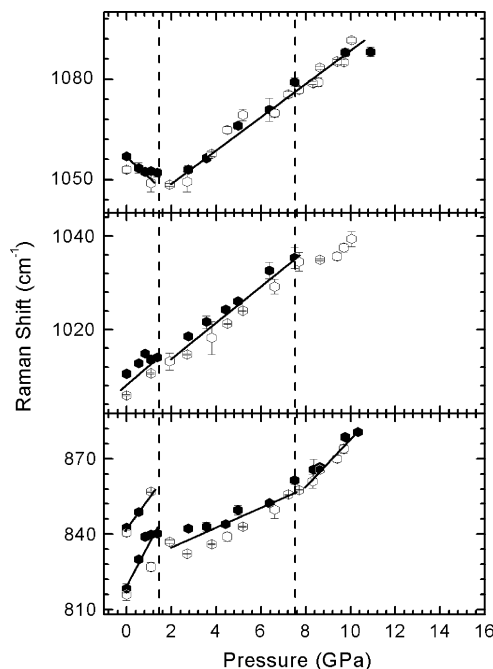


Figure 5. Vibrational mode associated with skeletal C–C stretching as a function of pressure. Filled symbols represent increasing pressure data, and open symbols represent reverse pressure data. The solid lines are linear fits through the data.

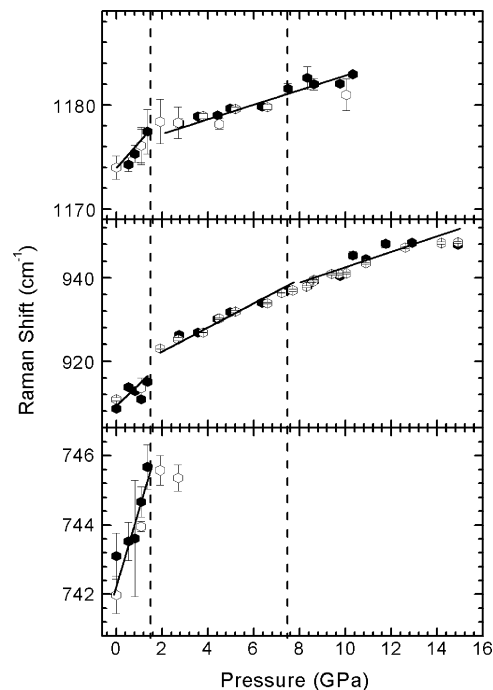


Figure 6. CH₂ vibration modes as a function of pressure. Filled symbols represent increasing pressure data, and open symbols represent reverse pressure data. The solid lines are linear fits through the data.

pressures leading to stiffening of these modes. The mode behavior is not affected by increase in pressure. This again suggests that the high-pressure phase III (>7.5 GPa) is not structurally very different from the low-pressure phase II (<7.5 GPa) except for changes along the *c*-axis.

3.2.5. CH₂ and CH₃ Bending. Figure 7 shows the CH₂ and CH₃ bending mode region and its pressure dependence. Both the symmetric and antisymmetric bending modes show a large pressure dependence as shown from the large $d\omega/dP$ values in Table 1. These modes persist up to 16 GPa and show changes

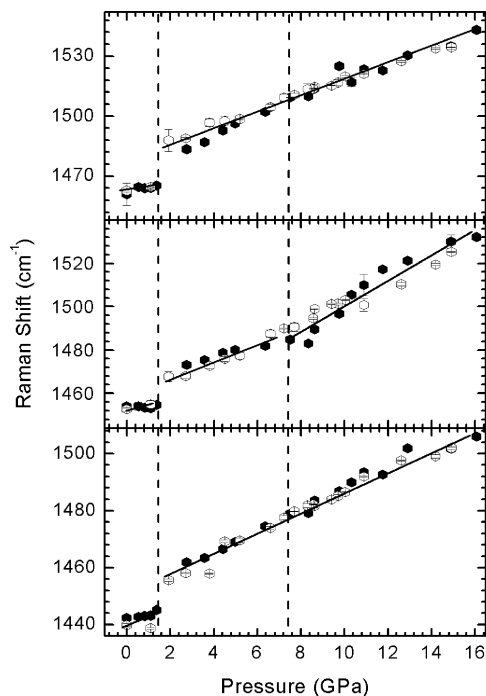


Figure 7. CH₂ and CH₃ bending modes as a function of pressure. Filled symbols represent increasing pressure data, and open symbols represent reverse pressure data. The solid lines are linear fits through the data.

in $d\omega/dP$ at both 1.5 and 7.5 GPa. The present behavior of these modes is due to reduced degree of freedom along the *c*-axis with decrease in volume at high pressure, which normally leads to stiffening of the modes. Like the C–C stretching and CH₂ vibrations, these modes remain up to 16 GPa and there is no considerable change in their character, suggesting that phase II (1.5–7.5 GPa) and phase III (>7.5 GPa) of *n*-heptane are structurally similar with subtle changes and dense packing along the *c*-axis.

Since the methyl end group experiences dampening, we propose that phase III is orientational disordered phase resulting due to different environments around the methyl end group. Such a transition is generally second order in nature. This is supported by our observations, viz., no hysteresis is observed around 7.5 GPa from our reverse pressure experiments as shown in Figures 2–7 by open symbol data.

In conclusion, high-pressure Raman spectroscopic studies on *n*-heptane carried out to 16 GPa suggest that *n*-heptane goes from a liquid to a solid state around 1.5 GPa. Upon further application of pressure in excess of 7.5 GPa *n*-heptane goes into a denser form, which is closely related to the earlier phase. The dampening of the rotational degree of freedom of methyl end group coupled with conversion of the gauche to trans

conformation at high pressures leads to the orientationally disordered phase at 7.5 GPa. The 7.5 GPa transition is a second-order transition as there is no hysteresis around this transition observed from our reverse pressure experiments. X-ray diffraction studies and theoretical studies would be able to throw more light on this.

Acknowledgment. We thank Balasubramaniam Sundaram and M. Krishnan for useful discussions. We also thank C. N. R. Rao and Ranga Uday Kumar for extending financial help for this work through research grants DRDO/CNR/4070 and SR/PF/340-A/2005-2006, respectively.

References and Notes

- (1) Dagaut, P.; Reuillon, M.; Cathonnet, M. *Combust. Sci. Technol.* **1994**, 95, 233.
- (2) Small, D. M. *The Physical Chemistry of Lipids*; Plenum Publishing: New York, 1988.
- (3) Chapman, D.; Jones, M.; Micelles, M. N. *Monolayers and Biomembrane*; John Wiley: New York, 1984.
- (4) Sirota, E. B.; King, H. E., Jr.; Hughes, G. J.; Wan, W. K. *Phys. Rev. Lett.* **1991**, 68, 492.
- (5) Ryckaert, J. P.; Klein, M. L.; McDonald, I. R. *Phys. Rev. Lett.* **1987**, 58, 698; *Mol. Phys.* **1994**, 83, 439.
- (6) Yamamoto, H.; Nemoto, N.; Tashiro, K. *J. Phys. Chem. B* **2004**, 108, 5827.
- (7) Guillaume, F.; Ryckaert, J. P.; Rodriguez, V.; MacDowell, L. G.; Girard, P.; Dianoux, A. J. *Phase Transitions* **2003**, 76, 823.
- (8) Boese, R.; Weiss, H. C.; Bläser, D. *Angew. Chem., Int. Ed.* **1999**, 38, 988.
- (9) Yamaguchi, M.; Serafin, S. V.; Morton, T. H.; Chronister, E. L. *J. Phys. Chem. B* **2003**, 107, 2815.
- (10) Krishnan, M.; Balasubramanian, S. *J. Phys. Chem. B* **2005**, 109, 1936.
- (11) Schoen, P. E.; Priest, R. G.; Sheridan, J. P.; Schnur, J. W. *J. Chem. Phys.* **1979**, 71, 317.
- (12) Snyder, R. G.; Strauss, H. L.; Alamo, R.; Mandelkern, L. *J. Chem. Phys.* **1994**, 100, 5422.
- (13) Olf, H. G.; Fanconi, B. *J. Chem. Phys.* **1973**, 59, 534.
- (14) Mao, H. K.; Bell, P. M. *Year Book—Carnegie Inst. Washington* **1978**, 77, 904.
- (15) Barnett, J. D.; Block, S.; Piermarini, G. J. *Rev. Sci. Instrum.* **1973**, 44, 1.
- (16) Kavitha, G.; Vivek, S. R. C.; Govindaraj, A.; Narayana, C. *Proc. Indian Acad. Sci. (Chem. Sci.)* **2003**, 115, 689.
- (17) Mayo, D. W.; Miller, F. A.; Hannah, R. W. *Course Notes on the Interpretation of Infrared and Raman Spectra*; John Wiley & Sons: New York, 2004.
- (18) Casal, H. L.; Mantsch, H. H.; Cameron, D. G.; Snyder, R. G. *J. Chem. Phys.* **1982**, 77, 2825.
- (19) Wong, P. T. T.; Mantsch, H. H.; Snyder, R. G. *J. Chem. Phys.* **1983**, 79, 2369.
- (20) Snyder, R. G.; Cameron, D. G.; Casal, H. L.; Compton, D. A. C.; Mantsch, H. H. *Biochim. Biophys. Acta* **1982**, 684, 111.
- (21) Brown, K. G.; Brown, E. B.; Ladjadj, M. *J. Phys. Chem.* **1987**, 91, 3436.
- (22) Wallach, D. F. H.; Verma, S. P.; Fookson, J. *Biochim. Biophys. Acta* **1979**, 559, 153.
- (23) Maroncelli, M.; Strauss, H. L.; Snyder, R. G. *J. Chem. Phys.* **1985**, 82, 2811.